to be presented at: AISTech 2011, Indianapolis, Indiana, May 2-5, 2011.

Effect of Nozzle Clogging on Surface Flow and Vortex Formation in the Continuous Casting Mold

Seong-Mook Cho, Seon-Hyo Kim
Pohang University of Science and Technology
Department of Materials Science and Engineering,
San31, Hyoja-Dong, Nam-Gu, Pohang, Kyungbuk 790-784, Republic of Korea
Phone: 82-54-279-5968
Fax: 82-54-279-2399
E-mail: y104401@postech.ac.kr

Rajneesh Chaudhary, Brian G. Thomas
University of Illinois at Urbana-Champaign
Department of Mechanical Science and Engineering
1206 West Green Street, Urbana, IL 61801
Phone: 217-333-6919
Fax: 217-244-6534
E-mail: bgthomas@uiuc.edu

Ho-Jung Shin
Korea Institute of Industrial Technology,
Resources Recycling Policy Office, Korea National Cleaner Production Center (KNCPC)
707-34 Yeoksam-Dong, Gangnam-gu, Seoul 135-918, Republic of Korea
Phone: 82-2-2183-1521
Fax: 82-2-2183-1529
E-mail: ceraby@kncpc.re.kr

Woong-Ryul Choi, Sung-Kwang Kim
POSCO
Continuous Casting Technology Development Team, Gwangyang Works
Gwang-yang, Junnam 545-711, Republic of Korea
Phone: 82-61-790-6404
E-mail: missko@posco.com

Keywords: continuous casting; asymmetric flow; entrapment; vortex; water model

ABSTRACT

Nozzle clogging induces asymmetric surface flow causing vortex formation and inclusion defects. This work applies computational and experimental approaches with a one-third scale water model of the process. Flow patterns are predicted with a three-dimensional $k-\varepsilon$ turbulent flow model. Surface velocity, flow-direction, and vortex formation location and frequency are measured at the surface of mold. Asymmetric clogging was investigated by making reductions in the size of one of the ports of the bifurcated nozzle. The resulting increase in the asymmetries of the surface flow velocities, velocity time variations, and vortex occurrence frequency on opposite sides of the mold are quantified.

INTRODUCTION

Continuous casting is used to manufacture over 90% of steel in the world [1], so understanding and optimizing the process is important to minimize defects in steel. Most of the defects affecting slab quality are associated with surface flow in the mold [2]. Asymmetric surface flow in the mold is one of the main phenomena attributed to cause inclusion entrainment [3-6] which can make "sliver" defects in the rolled product, caused by inclusions being trapped in the solidifying shell in the mold

Nozzle clogging is one of the severe problems that can induce asymmetric flow. The nozzle flow pattern can be changed by asymmetric flow through clogged regions, resulting in asymmetric flow in the mold. Asymmetric mold flow can cause faster surface flow on one side of the mold, causing level fluctuations, vortices [7-9] and instability of the interfacial layer between the molten steel and liquid mold flux [10]. These phenomena can entrain liquid mold flux into the molten steel, inducing entrapment of inclusions into the solidifying steel shell. On the other hand, slow surface flow can be induced on the opposite side, which results in abnormal low and nonuniform temperature, inducing nonuniform liquid mold flux layer thickness and serious problems during initial solidification.

Previous researchers have studied the causes and effects of nozzle clogging in continuous casting. Rackers and Thomas classified the types of clogs as: agglomeration of deoxidation products, solid steel build up, agglomeration of complex oxides and reaction product build up; and the types of transport mechanisms of oxidation products to the nozzle wall as: turbulent recirculation zones, turbulent flow, rough nozzle wall and external corners [11]. Several researchers studied clogging detection [12] and clogging prevention [13]. Bai and Thomas investigated the effects of clogging near the slide-gate on nozzle flow, and found that clogging affects both flow pattern and pressure drop [14]. Recently, Zhang et al. evaluated the nozzle port clogging on inclusion removal, slag entrainment, heat transfer and prediction of breakouts [15].

This work investigates the effect of nozzle clogging on fluid flow in the nozzle and mold using 1/3 scale water model experiments and computational modeling of the water model. Many previous successful studies of mold fluid flow have been done using water models [16-18] and computational modeling [19,20]. The current study applies water model experiments to quantify surface flow, vortex formation frequency, and computational modeling to explain the nozzle and mold flow pattern.

METHODLOGY

Water Model Experiments

Experiments were performed using a 1/3rd scale water model of the real continuous casting process, shown in Figure 1. The model consists of a tundish, stopper-rod, Submerged Entry Nozzle (SEN), and mold. Vertical movement of the stopper-rod controls the water flow rate from the tundish through the SEN into the mold, by changing the size of the annular gap between the stopper end and the bottom of the tundish where it curves into the SEN. Water exits holes in the bottom of the mold to a holding water bath and is pumped continuously back up to the tundish.

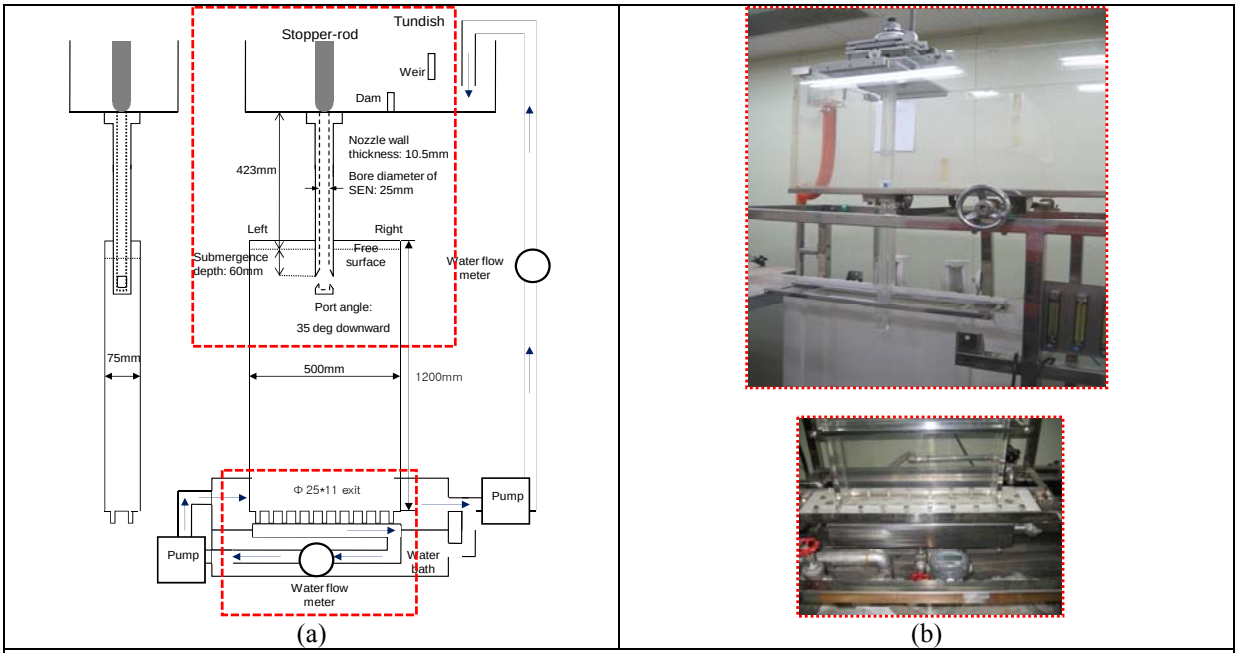

Figure 1. (a) Schematic, (b) Pictures of 1/3 scale water model

Single-phase flow was adopted, so the possible effects of argon gas-bubble injection were not studied. The three nozzles were adopted for investigating the nozzle clogging effects on surface flow and vortex formation as shown in Figure 2. These nozzles have typical bifurcated, 35-degree down-angled rectangular ports. Clogged nozzles have the cross-sectional areas of their left ports decreased by 33% (small-clog case) and 67% (severe-clog case) relative to the non-clogged right port. Further details are given in Table 1. Table 2 provides details of the casting conditions, nozzle and mold dimensions of this 1/3rd water model and real caster. Similarity between the 1/3 scale water model and the real caster conditions was determined based on maintaining a constant Froude number defined as the ratio of inertia force to gravitational force, $\mathbf{v} / \sqrt{\mathbf{gL}}$

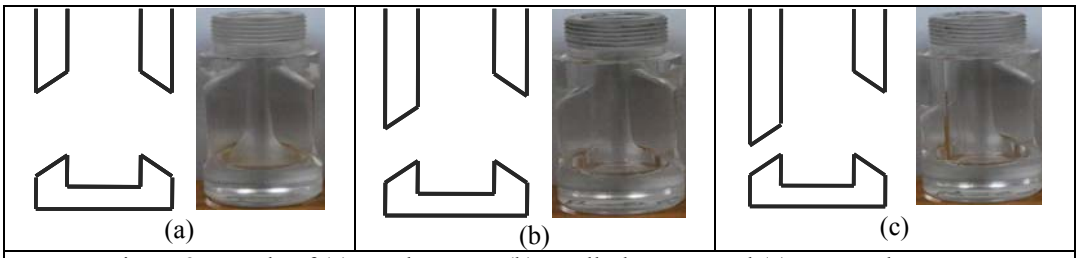

Figure 2. Nozzle of (a) no-clog case, (b) small-clog case and (c) severe-clog case

Table 1. Dimensions of nozzle ports

Left port			Right port
No-clog	Small-clog	Severe-clog	All cases
23.3mm × 26.7mm	19.0mm × 21.8mm	13.5mm × 15.4mm	23.3mm × 26.7mm

Table 2. Processing Conditions for Experimental and Computational Works

	1/3 scale water model	**Real caster**
Casting speed	**0.917 m/min**	**1.59 m/min**
Water flow rate	**34.4 LPM**	**537 LPM (3.77 Ton/min)**
Mold width	**500 mm**	**1500 mm**
Mold thickness	**75 mm**	**225 mm**
SEN depth	**60 mm**	**180 mm**
ρ_{fluid}	**998.2 kg/m^3 (water)**	**7020 kg/m^3 (steel)**
μ_{fluid}	**0.001003 kg/m-s (water)**	**0.0067 kg/m-s (steel)**
Nozzle (well-bottom type) port angle	**35 degree**	
Nozzle ports	**No-clog: Symmetric ports Small-clog: 0.67 asymmetric left port, Severe-clog: 0.33 asymmetric left port**	
Nozzle bore diameter (inner/outer)	**25 mm/46 mm**	**75mm/138mm**
Shell	**no**	**Yes**
Gas injection	**no**	**Yes**

Surface velocity measurements were performed using electromagnetic current sensor located at the five positions shown in Figure 3; 1/2L, 1/4L positions on each side (L: distance across the mold width from the narrow face to SEN center) and the center position (in the gap between SEN outer wall and wide face). The sensor was dipped at the above positions from the free surface to measure instantaneous velocity signal at 10mm below free surface. Instantaneous surface velocity data were collected for 1000sec at a collecting frequency of 1 Hz with 1 Hz of response time. The sensor has a circular cylinder head with 8mm diameter and 20mm height, which can measure surface velocity, including in the small gap between the SEN and mold as shown in Figure 4. Two components of horizontal surface velocity are measured; one parallel and one perpendicular to the mold width direction. Flow direction angle and velocity magnitude are determined from the velocity components, to quantify the surface flow vector

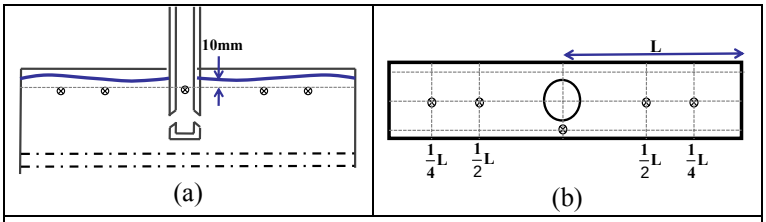

Figure 3. Locations of electromagnetic current sensor for measuring velocity

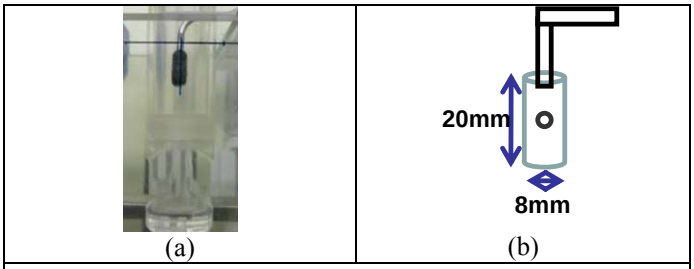

Figure 4. (a) Picture and (b) schematic of electromagnetic current sensor

To investigate nozzle clogging effects on vortex formation, sesame seeds were used as tracer particles for visualization and vortex phenomena were recorded with a video camera. Vortices were observed in four regions near the SEN, as shown in Figure 5. After recording, the number and location of all vortices lasting over 2 rotations were counted from the recorded video. The number of vortices in each region was divided by total measuring time (10 minutes) to calculate the local "frequency" of vortex formation.

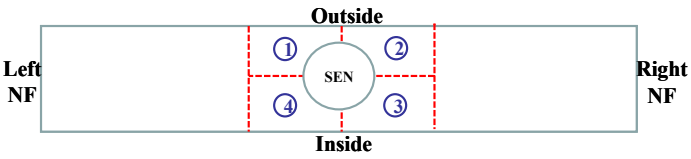

Figure 5. Regions where vortex formation was observed and counted

Computational modeling

A three-dimensional finite-volume computational model was applied to investigate the flow pattern in a nozzle and mold for the no-clog, small-clog and severe-clog cases. The steady-state, incompressible, Navier-Stokes equations with standard $k-\varepsilon$ model have been solved in the commercial computational fluid dynamics (CFD) package program, FLUENT to simulate the time-averaged turbulent flow. To decrease computer efforts, one-quarter nozzle and mold domains were used to simulate flow for the no-clog case along (4-fold symmetry) and half domains were used for the small- and severe-clog cases along (2-fold symmetry) as shown in Figure 6. Hexahedral cells were used for structured meshing of each domain; 107,356 cells with no-clog case, 206,304 cells with small-clog case and 202,610 cells with severe-clog case.

To obtain more accurate simulations of fluid flow in the mold, the SEN domain was connected with the mold domain and calculated together [15]. For inlet boundary conditions where flow enters the sides of a cylinder representing part of the tundish bottom,the normal velocity was applied to match the flow rate in the 1/3 scale water model, along with 10^{-5} m^2/sec^2 for turbulent kinetic energy and 10^{-5} m^2/sec^3 for turbulent dissipation rate. At the mold bottom, outlet boundary conditions of 0 pascal of gauge pressure, 10^{-5} m^2/sec^2 for turbulent kinetic energy and 10^{-5} m^2/sec^3 for dissipation rate were applied. The top surface of the mold was a stationary wall with 0 pascal shear stress components for free-slip boundary condition. For all three cases, convergence of solving the equations was defined when all scaled residuals were stably reduced below 10^{-4}.

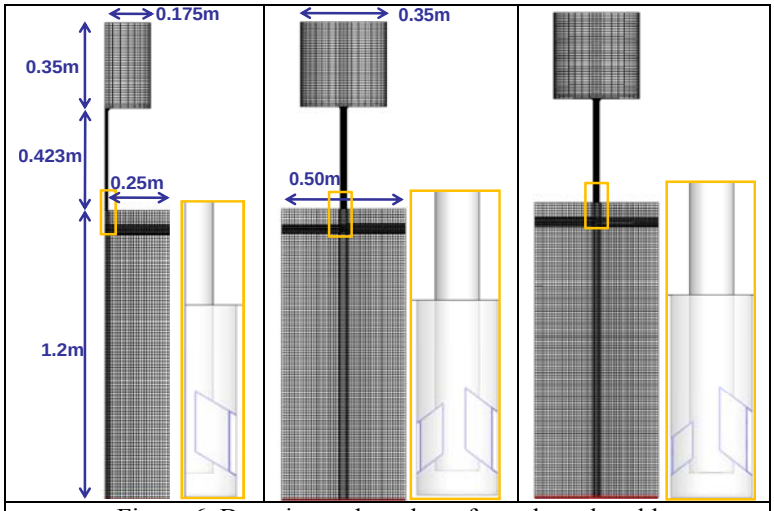

Figure 6. Domains and meshes of nozzle and mold

NOZZLE FLOW

To investigate the effects of nozzle port clogging on nozzle flow, velocity magnitude contours and streamlines are presented in Figure 7 for the three cases. The two clog cases have "small" clogging with the left port 33% smaller than the right port and "severe" clogging with the left port 67% smaller. The asymmetric port size causes asymmetric flow through the ports. The small-clog case has only 48% of the total flow rate exiting through the clogged left port. Severe clogging is much more asymmetric, with only 25% of the flow rate exiting through the clogged left port. Furthermore, higher velocity is induced through the non-clogged port, which causes higher momentum flow towards the right side of the mold. The back flow usually observed at the top of these oversized ports is not found in the clogged left port, which has low flow rate, low velocity, and a more uniform velocity profile.

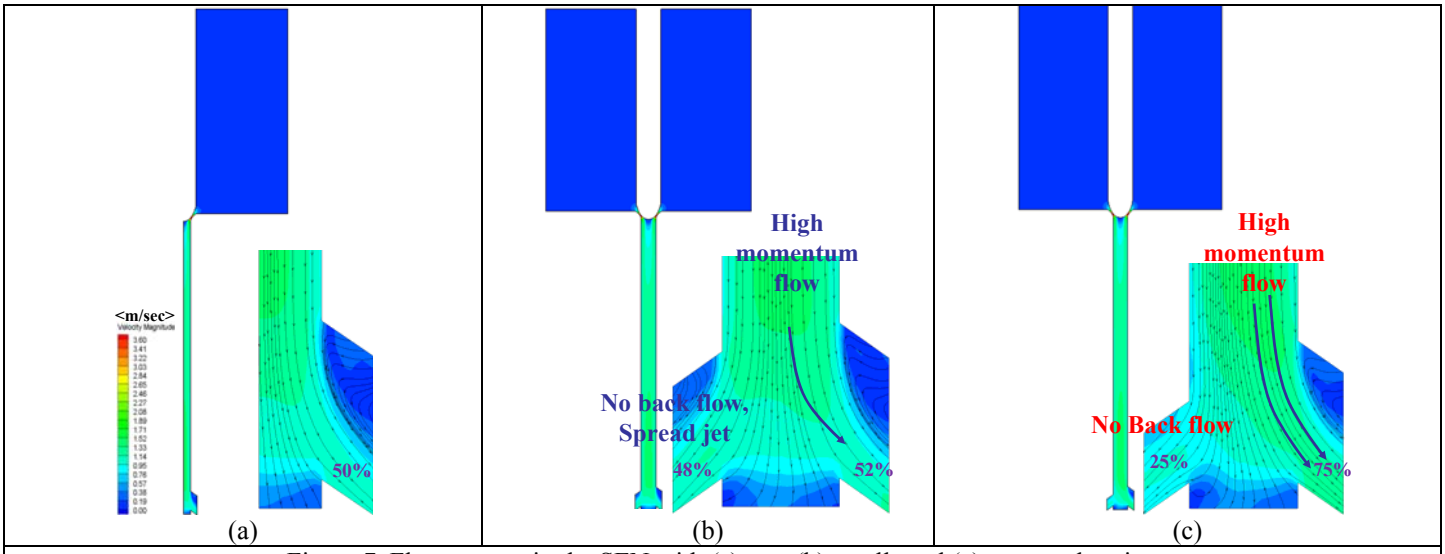

Figure 7. Flow pattern in the SEN with (a) no-, (b) small- and (c) severe-clogging

Table 3 shows the jet characteristics leaving each nozzle port. As expected, increasing asymmetry of the port sizes causes increased asymmetry of jet velocity, jet angle, turbulent kinetic energy and turbulent kinetic dissipation rate. The vertical jet angle becomes larger (directed more steeply downwards) at the non-clogged port and smaller at the clogged port, relative to the average vertical jet angle with no clogging. The difference in vertical jet angle between the left and right port increases from 5.2 degree in small-clog case to 6.9 degree in severe-clog case. Average jet force is calculated by multiplying the flow rate and average jet speed. Total jet force from both ports increases with nozzle clogging. Asymmetry of jet force between the left and right ports increases with more clogging, from 12% difference with small-clogging to 58% difference with severe-clogging.

Table.3 Jet characteristics

	No-clog		Small-clog		Severe-clog	
	Left	Right	Left	Right	Left	Right
Weighted average nozzle port velocity in x-direction (Outward) (m/sec)	0.450	0.451	0.568	0.550	0.542	0.636
Weighted average nozzle port velocity in y-direction (Horizontal) (m/sec)	0.042	0.042	0.017	0.009	0.022	0.015
Weighted average nozzle port velocity in z-direction (Downward) (m/sec)	0.315	0.315	0.343	0.404	0.327	0.497
Vertical jet angle (degree)	-35.0	-35.0	-31.2	-36.4	-31.1	-38.0
Horizontal jet angle (degree)	0	0	0	0	0	0
Average jet speed(m/sec)	0.55	0.55	0.66	0.68	0.63	0.81
Flow rate (kg/sec)	0.286 (50%)	0.286 (50%)	0.276 (48%)	0.296 (52%)	0.145 (25%)	0.427 (75%)
Averaged jet force (N)	0.157	0.157	0.182	0.201	0.091	0.346
Maximum velocity magnitude (m/sec)	0.98	0.98	1.10	1.17	0.87	1.28
Weighted average turbulent kinetic energy(m^2/s^2)	0.022	0.022	0.043	0.020	0.033	0.019
Weighted average turbulent kinetic energy dissipation rate (m^2/s^3)	0.782	0.783	2.12	0.797	1.47	0.731
Back-flow zone (%)	17.2	17.2	0	16.9	0	17.2

MOLD FLOW PATTERN

Asymmetric jet flow from the nozzle due to partial clogging of one port induces asymmetry of the mold flow pattern, causing an unbalanced double roll pattern, shown in Figure 8. With clogged nozzles, strong surface flow from the right narrow face crosses sides to suppress the uprising flow from the left narrow face. This decreases the size of the upper circulation region at the left side, where the port is partly clogged. In the severe-clog case, the flow does not rise upward after hitting left narrow face, due to the high strength of this cross flow coming from other side. The faster flow from the non-clogged side in this severe clog case generates strong upward and downward flows after hitting the right narrow face. The strong upward flow can be detrimental in shearing off liquid slag from the top surface. The strong downward flow can be detrimental by taking inclusions deep into the mold cavity along the right narrow face, inducing more internal defects. This inbalanced flow behavior in the mold is consistent with the nozzle flow explained with the help of jet angle and jet force in the previous section.

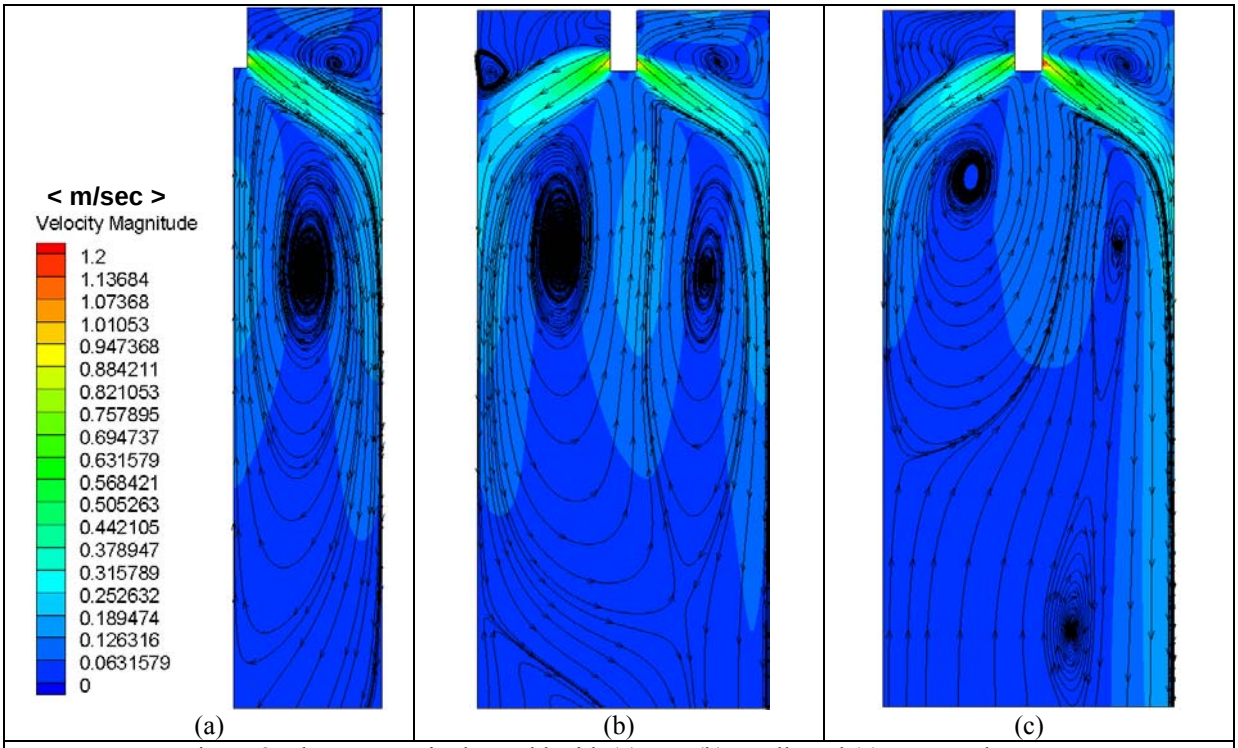

Figure 8. Flow pattern in the mold with (a) no-, (b) small- and (c) severe- clog case

SURFACE FLOW VELOCITY

To investigate nozzle clogging effects on instantaneous surface flow, the electromagnetic current sensor is used to measure the two horizontal components of instantaneous surface velocity at five places on the surface of the mold as a function of time. Flow direction angle, θ, as defined in Figure 9, is determined by arctangent calculation from two velocity components. Note that the coordinate axis definition for this calculation changes between mold sides.

The unbalanced mold flow pattern induces asymmetric surface flow, as shown in Figures 10 and 11. Each graph shows the time variation of the velocity magnitude (black lines) and direction angle (blue lines) of the surface flow. Figure 10 sequentially shows the results at the 1/4 width location from the left narrow face, 1/2 width location from left narrow face, 1/2 width location from right narrow face and 1/4 width location from right narrow face. Results in the gap between SEN outer wall and mold inner wall are shown in Figure 11.

Surface flow becomes slower and more chaotic toward SEN in both sides with non-clogged nozzle. This trend of velocity magnitude and direction angle of surface flow is same with clog cases. Nozzle clogging makes faster and more consistent surface flow from right NF same side with non-clogged port than left NF same side with clogged port. The faster surface flow is caused by more force of jet flow from non-clogged port, which result in more faster uprising flow after impinging at the narrow face. On the other side, surface flow at the left (slower) side is more chaotic than right side showing the large fluctuation of flow direction angle, and this trend is severe with more clogging. More asymmetrical flow between left and right side makes faster flow in the gap between SEN and mold. The flow in the gap with more clogged nozzle has more consistent direction angle with higher velocity.

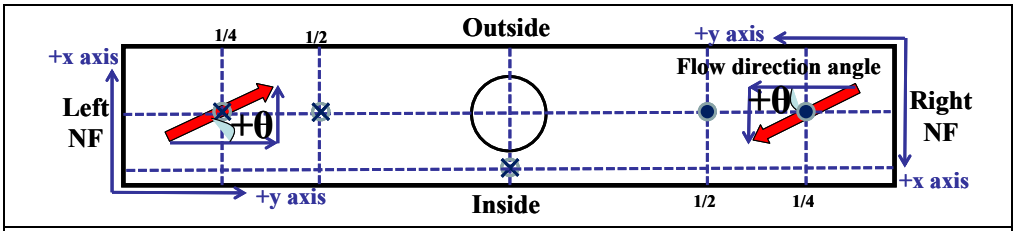

Figure 9. Definition of flow direction angle on both sides of SEN

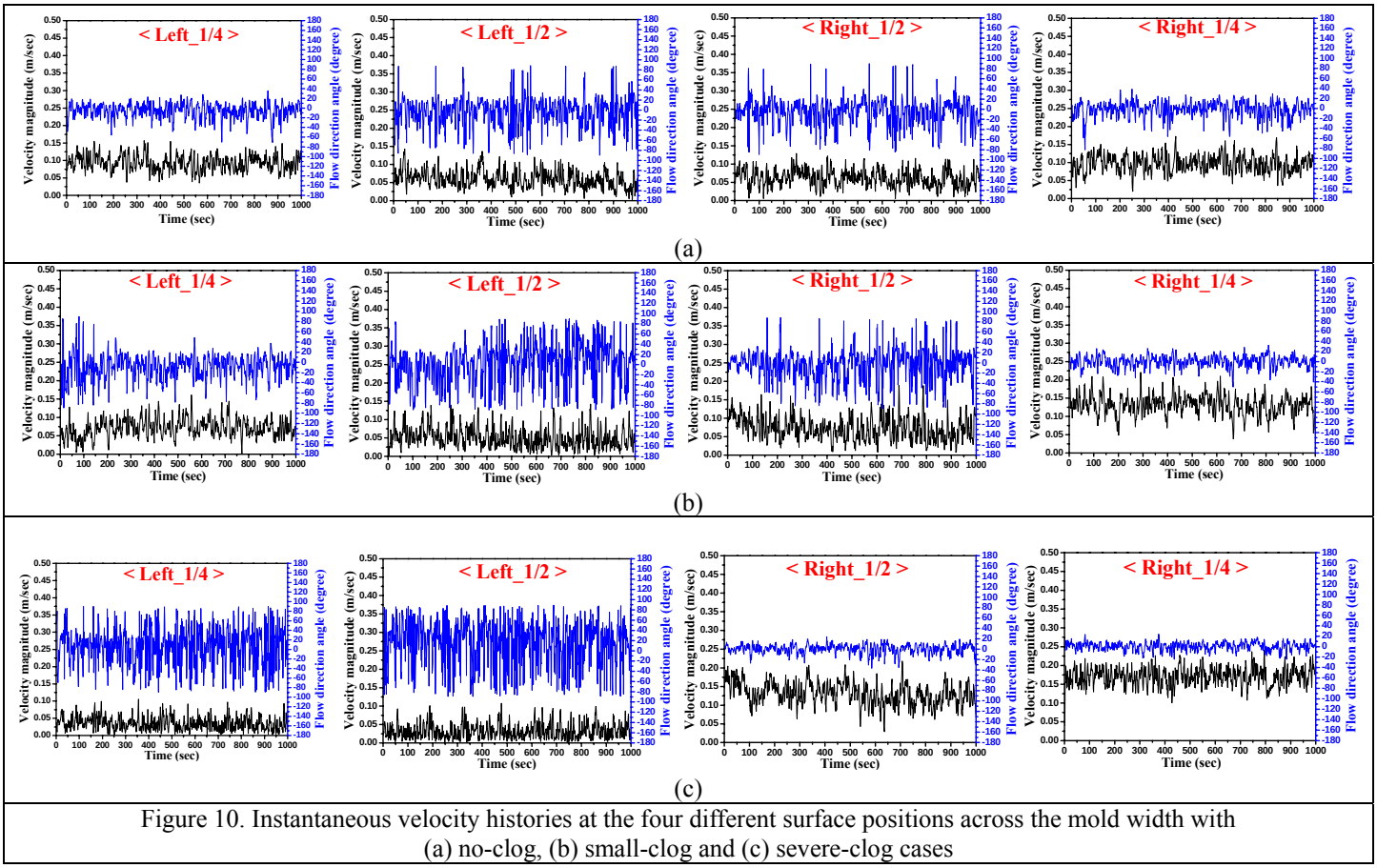

Figure 10. Instantaneous velocity histories at the four different surface positions across the mold width with (a) no-clog, (b) small-clog and (c) severe-clog cases

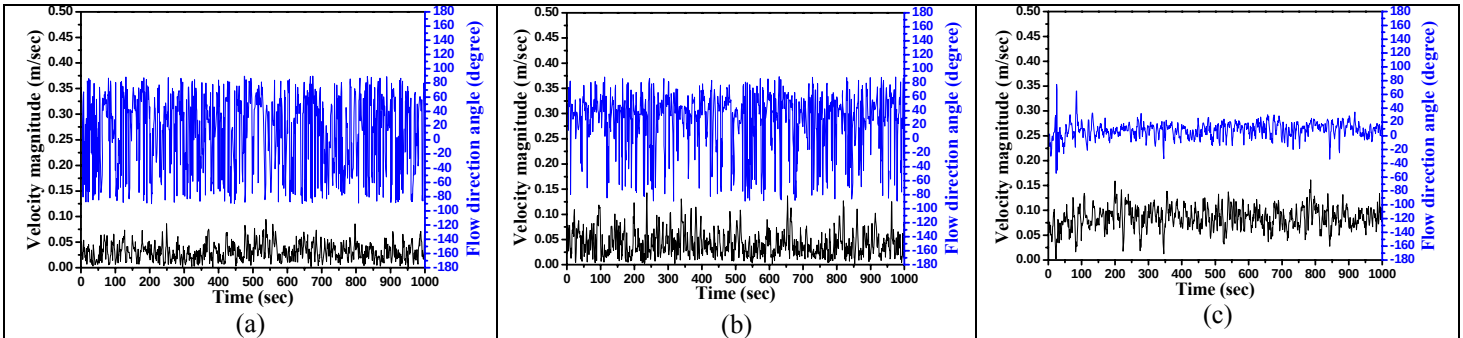

Figure 11. Instantaneous velocity histories through the surface center (gap between SEN and mold) with (a) no-clog, (b) small-clog and (c) severe-clog case

Figure 12 shows the time-average flow pattern, including the measured velocity vectors and magnitudes (top) and calculated speed contours and streamlines (bottom). As shown in the instantaneous velocity histories in Figures 10 and 11, nozzle clogging causes asymmetry of the average surface flow in the mold. Flow at the right (non-clogged) side is faster than the left (clogged port) side, causing more flow towards the left narrow face, and faster flow in the gap between SEN and mold. With no clogging, flow in the gap is directed toward the wide face, as the surface flows impinge from both sides. This is quite realistic and physically consistent since its

a symmetry and normal velocity should be zero. With a clogged left port, the stronger surface flow from the right side overcomes flow from the left side. This causes consistent flow through the gap towards the left side with clogging.

The measured and predicted surface flow directions differ at the left side of the mold. In the small-clog case, the flow direction at 1/2 L position of left side is predicted towards the left narrow face. Surface flow direction with severe-clog case is totally directed towards the left side. This over-prediction of the severity of the surface asymmetry is caused by a slight over-prediction of the ½ L surface velocity on the right side, and the corresponding extra momentum that suppresses the left side flows. As shown in Figure 13, the surface velocity is predicted to be greatest at the ½ L location, but the measurements are greatest at the ¼ L location. These differences between simulations and measurements are likely due to the inability of this simple steady state turbulence model to capture the complex transient vortexing flow.

In spite of this over-prediction of surface flow asymmetries between right and left, the predictions match reasonably well with the measurements of surface velocity, as shown in Figure 13. Nozzle clogging clearly induces strong asymmetric surface flow in the mold. Surface flow at the side of the mold with the non-clogged port is faster than the clogged-port side. More flow asymmetry between left and right sides induces faster flow in the gap between SEN and mold.

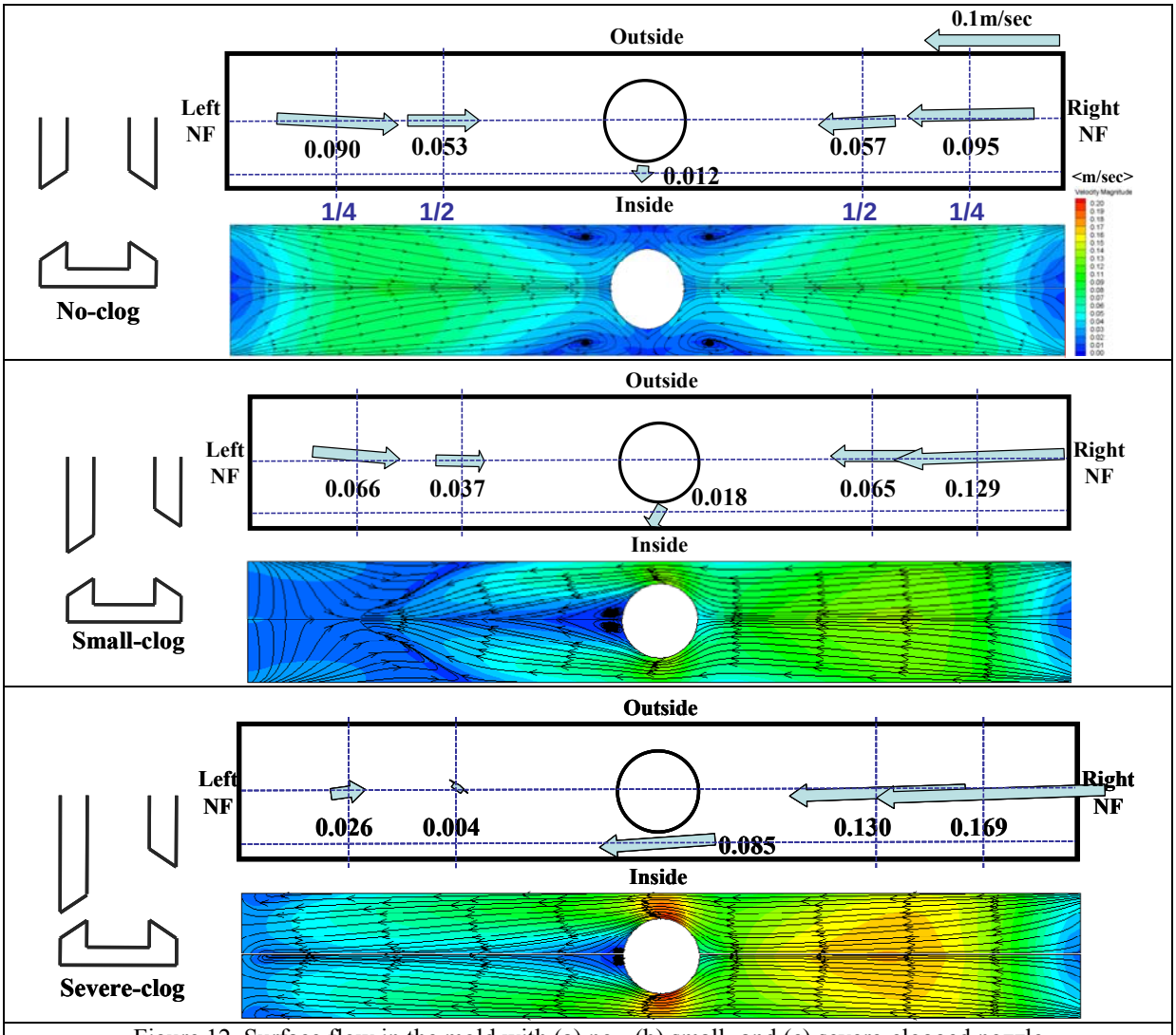

Figure 12. Surface flow in the mold with (a) no-, (b) small- and (c) severe-clogged nozzle

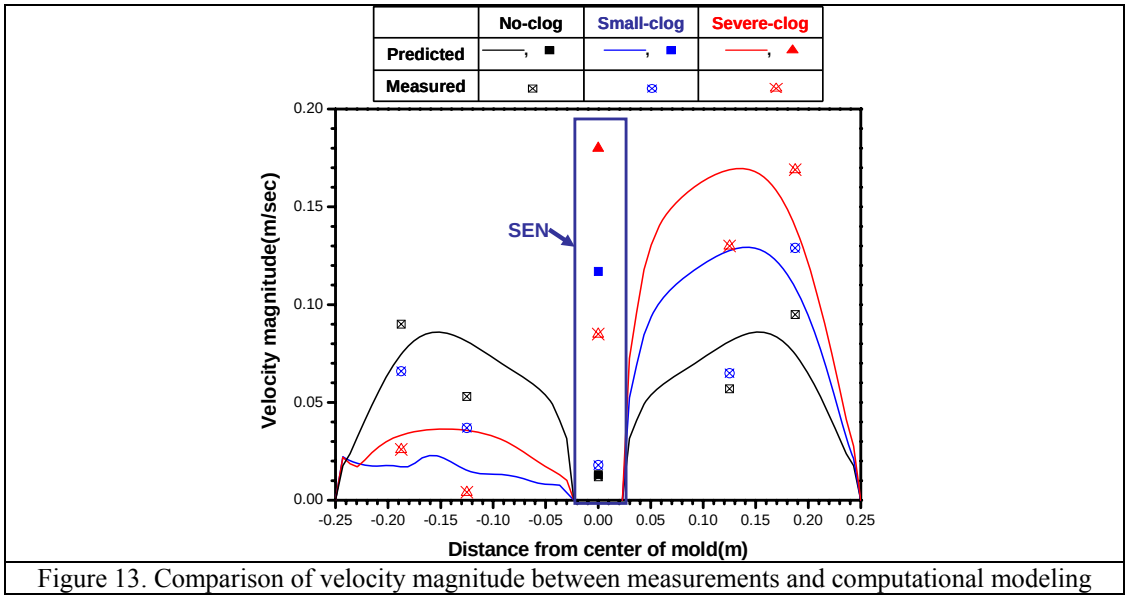

Figure 13. Comparison of velocity magnitude between measurements and computational modeling

VORTEX FORMATION

Almost all vortices form within 60mm from the mold center in the four regions defined in Figure 5. Vortices at 1st and 3rd region rotate counter-clockwise and at 2nd and 4th region rotate clockwise, as shown in Figure 14. The number printed in each of the four regions is vortex formation frequency, calculated by counting how many vortices formed during 10 minutes. As expected, nozzle clogging causes asymmetric vortex formation with more vortices at the left side of the SEN. This is caused by more consistent and faster flow toward the left side through the gap between SEN outer wall and mold inner wall. In addition, more chaotic and slower flow at the 1/2L location could be induced by vortex formation near SEN. Thus, variations of flow direction angle are more severe with increased clogging at the 1/2L location due to the increased vortices.

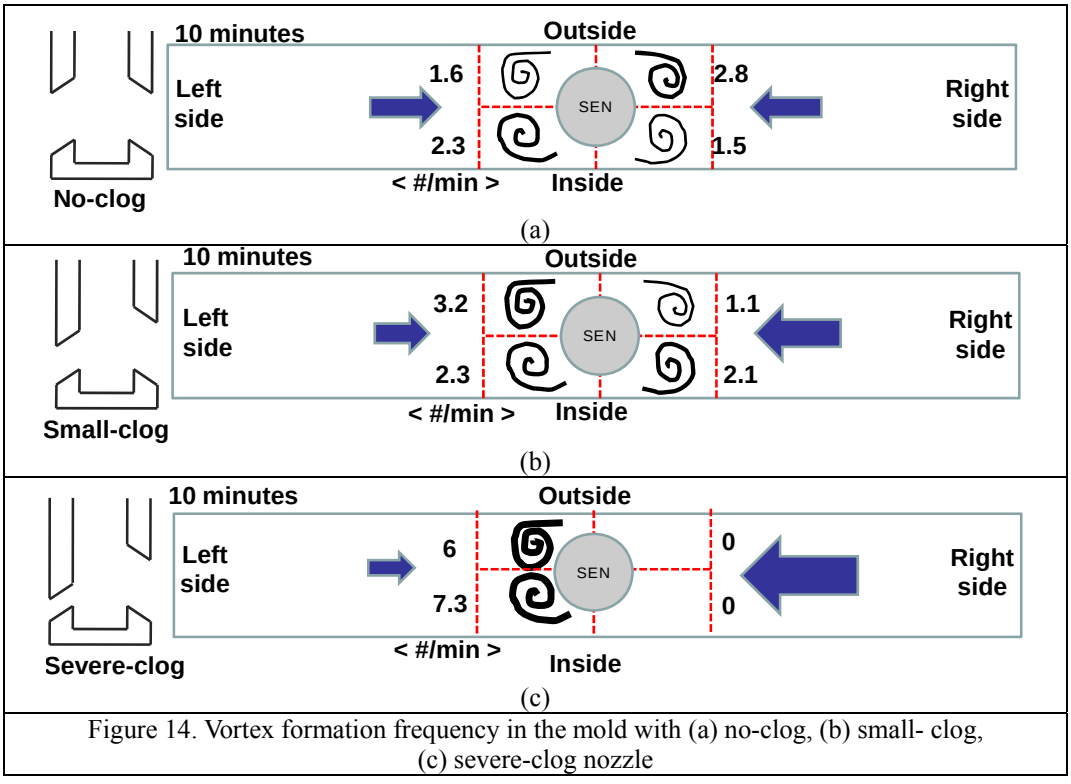

Figure 14. Vortex formation frequency in the mold with (a) no-clog, (b) small- clog, (c) severe-clog nozzle

The frequency of occurrence of vortices at the left (1st and 4th) regions are added and compared with the vortex frequency at the right (2nd and 3rd) regions in Figure 15(a) and Table 4 to show the effect of left-right asymmetric flow caused by nozzle clogging. As

expected, significant asymmetry is observed in the clog cases having asymmetric nozzle ports size, and more severe with more clogging. Similarly, the vortex formation frequencies at the inside (3rd and 4th) regions are added and compared with the vortex frequency at the outside (1st and 2nd) regions in Figure 15(b) and Table 5 to show the effect of asymmetric flow by nozzle clogging on inside-outside asymmetry. As expected, asymmetry between vortex formation frequency on inside and outside radius locations is not significant in these 3 cases. Minor differences are likely due to the limitations of the vortex formation frequency measurement method and a need for longer time averaging. Significantly more (26% more) vortices are observed on the left side for the small-clog case, and all vortices are formed to the left of the SEN with the severe-clog case. These vortices are caused by the velocity difference between the left and right side, which causes flow through the gap between the SEN and the mold, and vortex shedding on the downstream side. Furthermore, clogging increases vortex formation. Specifically, the total vortex frequency increases by 7% with small-clog case and 62% with severe-clog case relative to 8.2 /min with no clogging. Even with a non-clogged nozzle, many vortices are observed. These are due to random velocity variations between left and right sides, caused by turbulence in the mold.

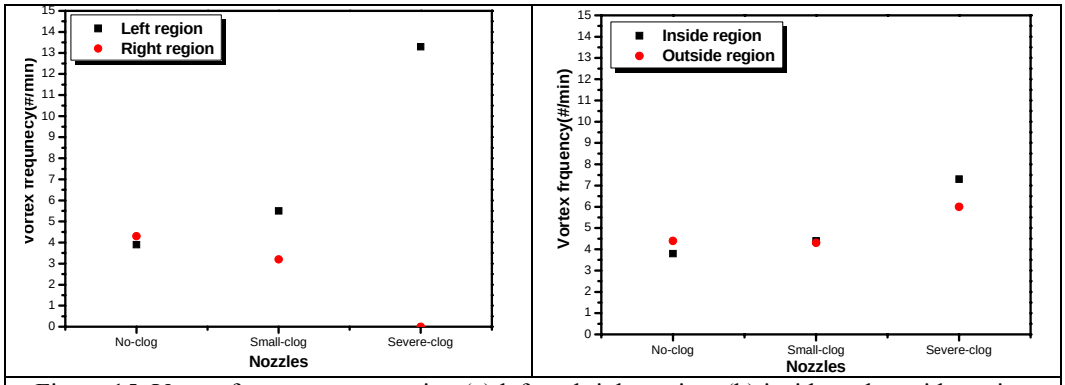

Figure 15. Vortex frequency comparing (a) left and right region, (b) inside and outside region

Table 4. Comparison of vortex frequency between left and right region

Vortex frequency(#/min)	Left	Right	Total
No-clog	3.9 (48%)	4.3 (52%)	8.2
Small-clog	5.5 (63%)	3.2 (37%)	8.7
Severe-clog	13.3 (100%)	0	13.3

Table 5. Comparison of vortex frequency between inside and outside region

Vortex frequency(#/min)	No-clog	Small-clog	Severe-clog
Outside	4.4 (54%)	4.3 (49%)	6 (45%)
Inside	3.8 (46%)	4.4 (51%)	7.3 (55%)
Total	8.2	8.7	13.3

CONCLUSIONS

Nozzle clogging effects on nozzle and mold flow have been studied with 3 cases of clogging (No-clog, Small-clog and Severe-clog). The results are summarized in Figure 16.

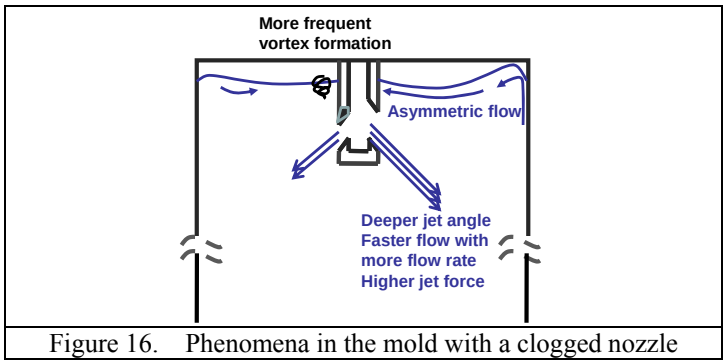

Figure 16. Phenomena in the mold with a clogged nozzle

- Asymmetrical port size due to clogging causes asymmetric flow rate, velocity, turbulent kinetic energy, dissipation rate and jet force, resulting in asymmetric jet flow between sides.
- Increased, faster flow from the non-clogged nozzle port causes a deeper jet angle and higher force than from the clogged port, which causes asymmetric flow and an unbalanced double roll pattern in the mold.

- With severe clogging, the strong upward flow on the non-clogged side could shear liquid slag from the top surface, and the strong downward flow could penetrate inclusions deep into the mold cavity, causing internal defects.
- Surface flow always becomes slower and more chaotic towards the SEN, due to vortices forming in four regions near the SEN.
- With clogging, surface flow across the side with the non-clogged port is faster than with the clogged port. This stronger surface flow can cross the gap to suppress flow on the other side, and creates vortices.
- Vortices are caused by asymmetric flow between right and left sides through the gap between the SEN and mold widefaces.
- More clogging causes more asymmetry of flow between the two sides.
- More clogging causes faster gap flow, and more vortices near the SEN on the side of the mold with the clogged port.
- The steady-state standard $k-\varepsilon$ model shows a reasonable quantitative match with the measurements. This model over-pridicts the asymmetric suppression of surface flow by the faster non-clogged side. The limited accuracy of this steady state model is perhaps due to complex transient vortexing flow. More accurate transient models, such as LES, are needed to improve model predictions.

ACKNOWLEDGEMENTS

The authors thank POSCO and Shin-Eon Kang, POSCO Technical Research Laboratories for providing the water model. Support from the Continuous Casting Consortium, University of Illinois at Urbana-Champaign, POSCO, South Korea (Grant No. 4.0006378.01) and the National Science Foundation (Grant No. DMI 07-27620) is gratefully acknowledged.

REFERENCES

1. Wolf, M.M., History of Continuous Casting, in Steelmaking Conf. Proc. 1992, Iron & Steel Society, Toronto, Canada. p. 83-137.
2. Thomas, B.G. and S.P. Vanka, "Study of Transient Flow Structures in the Continuous Casting of Steel", NSF Design & Manufacturing Grantees Conference, Vancouver, Canada: NSF, Washington, D.C, 2000
3. Miki, Y. and S. Takeuchi, Internal defects of continuous casting slabs caused by asymmetric unbalanced steel flow in mold. ISIJ Int., 2003. 43(10): p. 1548-1555.
4. Zhang, L.F., et al., Investigation of fluid flow and steel cleanliness in the continuous casting strand. Metallurgical and Materials Transactions B-Process Metallurgy and Materials Processing Science, 2007. 38(1): p. 63-83.
5. Gupta, D., S. Chakraborty, and A.K. Lahiri, ISIJ Int., 1997. 37(7): p. 654-658.
6. Rajneesh Chaudhary, Go-Gi Lee, Brian G. Thomas, Seong-Mook Cho, Seon-Hyo Kim, Oh-Duck Kwon, "Effect of Stopper-Rod Misalignment on Fluid Flow in Continuous Casting of Steel", Metallurgical and Materials Transactions B, 'In press'
7. Li, B. and Tsukihashi, Vortexing flow patterns in a water model of slab continuous casting mold. ISIJ Int., 2005. 45(1): p. 30-36
8. Kasai and Iguchi, Water-model experiment on melting powder trapping by vortex in the continuous casting mold. ISIJ Int., 2007.47(7) p. 982-987
9. S.-M Cho, G.-G Lee, S.-H Kim, R. Chaudhary, O.-D Kwon, and B.G Thomas, "Effect of Stopper-Rod Misalignment on Asymmetric Flow and Vortex Formation in Steel Slab Casting", Jim Evans Honorary Symposium, in Proceedings of The Minerals, Metals, and Materials Society Annual Meeting 2009, The Minerals, Metals, and Materials Society, Vol.139, 2009, p.71-77
10. Lance C. Hibbeler and Brian G. Thomas, "Investigation of Mold Flux Entrainment in CC Molds Due to Shear Layer Instability", AISTech Proceedings, 2010
11. K. G Rackers and B. G. Thomas, "Clogging in Continuous Casting Nozzles", 78th Steel Conference Proceedings, Iron and Steel Society, Vol. 78, 1995, p.723-734
12. F.L Kemeny, "Tundish Nozzle Clogging – Measurement and Prevention", McLean Symposium Proceedings, Iron and Steel Society, 1998, p.103-110
13. Brian G. Thomas and Hua Bai, "Tundish Nozzle Clogging - Application of Computational Models", 18th Process Technology Division Conference Proceedings, Iron and Steel Society, Vol.18, 2001, p.895-912
14. Hua Bai and B. G Thomas, "Effects of Clogging, Argon Injection, and Continuous Casting Conditions on Flow and Air Aspiration in Submerged Entry Nozzles", Metallurgical and Materials Transactions B, Vol. 32B, 2001, p.707-722
15. Lefeng Zhang, Yufeng Wang and Xiangjun Zuo, "Flow Transport and Inclusion Motion in Steel Continuous-Casting Mold under Submerged Entry Nozzle Clogging Condition", Metallurgical and Materials Transactions B, Vol. 39B, 2008, p.534-550
16. B.G. Thomas, in Making, Shaping and Treating of Steel, 11th ed., vol. 5, Casting volume, A. Cramb, ed., AISE Steel Foundation, Pittsburgh, PA, 2003, pp.14.1-14.41
17. B.G. Thomas, X. Huang, and R.C. Sussman, Metall. Mater. Trans.B, 1994,vol. 25B, pp. 527-47
18. B.G. Thomas and L. Zhang, ISIJ Int., 2001, vol.41(10),pp.1181-93
19. QUAN YUAN, SIVARAJ SIVARAMAKRISHNAN, S.P. VANKA, and B.G. THOMAS, "Computational and Experimental Study of Turbulent Flow in a 0.4-Scale Water Model of a Continuous Steel Caster", Metallurgical and Materials Transactions B, 2004, Vol.35B, p.967-982
20. PÁVEL RAMÍREZ-LÓPEZ, R.D. MORALES, R. SÁNCHEZ-PÉREZ, L.G. DEMEDICES, and O. DÁVILA, "Structure of Turbulent Flow in a Slab Mold", Metallurgical and Materials Transactions B, 2005, Vol.36B, p.787-800